Using the Hybrid Kurtosis-based Method to Correlate Strain and Vibration Signals

S. ABDULLAH, N. ISMAIL, M. Z. NUAWI, M. Z. NOPIAH & A. ARIFFIN
Department of Mechanical and Materials Engineering,
Universiti Kebangsaan Malaysia,
43600 UKM Bangi, Selangor,
Malaysia.
shahrum1@gmail.com

Abstract: - This study specifically focuses on the coil spring, one of the automotive suspensions system parts. Under its service life, this component will be driven over different surface profiles that will give different displacements and vibration responses. This paper explores the correlation between the strain signals resulting from displacement and vibration responses when subjected to the variable amplitude loading. This comparative study was implemented using strain-life approach, (ε-N) and Hybrid Integrated Kurtosis-based Algorithm for Z-notch filter Technique (Hybrid I-kaz). The Hybrid I-kaz method provides a two dimensional graphical representation of the measured strain and vibration signal and Hybrid I-kaz coefficient, Z_h^{∞} in order to measure the degree of data scattering. An experiment has been performed on an automotive suspension system machine. This study was considered test signals which were excited based on ten different frequencies that were varied from 1 Hz to 10 Hz. A strain gauge of 5 mm in size and an accelerometer were mounted on the inner surface of the coil spring to measure the strain signals and vibration responses due to the loading. The time domain strain signals and vibration signals were then analysed based on the Coffin-Manson model for fatigue damage prediction and the Hybrid I-kaz method. The total fatigue damage and Hybrid I-kaz coefficients, Z_h^{∞} for each signal of the different frequencies were compared in order to perform the correlation study. From the analysis, it was found that the strain signal was linearly proportional to the vibration responses.

Key-Words: - Fatigue, Vibration response, Random loading, I-kaz Hybrid, Coefficient, Correlation

1 Introduction

In service life, automotive suspension system experiences the significant load that cause vibration and displacement that contributing to mechanical failure through fatigue [1]. Vehicle vibration may actually be due to an improperly functioning of automotive suspension system. Both strain and vibration signals are important parameters to achieve higher quality level of vehicles in term of ride comfort and resistant to high load [2]. Thus, it is worthy to study the relationship of these two parameters.

The strain and vibration signals measured on a coil spring were used as the subject of this study as this component directly experienced the load when the vehicle was driven over the road.

A vehicle was influenced by the excitations due to the road unevenness. The vehicle responses changed at the different velocities although the road condition remained constant. This factor was taking into consideration to induce different displacements and vibrations of the coil spring under it service conditions.

The analysis to be performed for the purpose of this paper is fatigue damage assessment. The strain-life approach (ε-N) was used for the fatigue damage analysis as this case study was related to low cycle fatigue, which is a suitable approach to analyse random data collected from automotive components [3].

Another analysis to be performed in this paper is statistical analysis, which is using the newly developed statistical-based method, called Hybrid Integrated Kurtosis-based Algorithm for Z-notch filter Technique (Hybrid I-kaz). Hybrid I-kaz method calculates the related coefficient for the measured signal that is called the Hybrid I-kaz coefficient, Z_h^{∞} and two dimensional graphic displays of the magnitude distribution.

This work assessed the total fatigue damage (D) and Z_h^{∞} of the strain and vibration signals at different frequencies. The goal was to determine the correlation between the strain and vibration signal of the coil spring in term of D and Z_h^{∞}.

2 Literature Review

2.1 Total fatigue damage

Three major approaches have widely been used to analyse fatigue damage or fatigue life, namely the stress-life approach (*S*-*N*), the strain-life approach (*ε*-*N*) and the linear elastic fracture mechanics (*LEFM*) [4]. However, the strain-life approach (*ε*-*N*) is used for the analysis as the case study was related to low cycle fatigue, which is a suitable approach to analyse random data collected from automotive components.

The strain-life approach considers the plastic deformation that occurs in the localised region where fatigue cracks begin under the influence of a mean stress. This approach is often used for ductile materials at relatively short fatigue lives. This approach is also used where there is little plasticity at long fatigue lives. Therefore, this is a comprehensive approach that can be used in place of the stress-based approach. Consequently, it is common that the service loadings caused by machines and vehicles is evaluated using a strain-life fatigue damage approach [5-10].

The foundation of the strain-life approach is the Coffin-Manson relationship [11, 12] and it is defined as the following equation

$$\varepsilon_a = \frac{\sigma'_f}{E}\left(2N_f\right)^b + \varepsilon' f\left(2N_f\right)^c \tag{1}$$

The majority of material fatigue data is collected in the laboratory by means of testing procedures which employ fully reversed loadings. However, some of the realistic service situations involve non-zero mean stresses. Therefore, it is extremely important to know the influence of the mean stress, so that the fully reversed laboratory data can be usefully employed in the assessment of real situations. Two mean stress effect models are commonly used, i.e. the Morrow and Smith-Watson-Topper (SWT) strain-life models. Morrow (1968) was the first to propose a modification to the base-line strain-life curve which accounted for the effect of the mean stress by modifying the elastic part of the strain-life curve. The Morrow's strain-life model [13] is mathematically defined by

$$\varepsilon_a = \frac{(\sigma'_f)}{E}\left(1-\frac{\sigma_m}{\sigma'_f}\right)\left(2N_f\right)^b + \varepsilon'_f\,(2N_f)^c \tag{2}$$

The SWT strain-life model [14] is mathematically expressed by

$$\varepsilon_a\sigma_{mak} = \frac{(\sigma'_f)}{E}(2N_f)^{2b} + \sigma'_f\,\varepsilon'_f\,(2N_f)^{b+c} \tag{3}$$

For all those three strain-life expressions, E is the material modulus of elasticity, ε_a is a true strain amplitude, $2N_f$ is the number of reversals to failure, σ'_f is a fatigue strength coefficient, b is a fatigue strength exponent, σ_{max} is a maximum fatigue stress, ε'_f is a fatigue ductility coefficient and c is a fatigue ductility exponent.

The fatigue damage caused by each cycle is calculated in reference to material life curves, i.e. stress life (*S*-*N*) or strain life (*ε*-*N*) curves. The N_f value for each cycle can be obtained from Eq. (1) to (3), and the fatigue damage value, D, for one cycle is calculated as

$$D = \frac{1}{N_f} \tag{4}$$

The total damage caused by N cycles is referred to the Palmgren-Miner rule, for which the accumulated damage, ΣD, is expressed as

$$\Sigma D = \sum \frac{N_i}{N_f} \tag{5}$$

Where N_i is the number of cycles within a particular stress range and mean, and N_f is the number of cycles to failure for a particular stress range and mean.

2.2 Statistical Analysis

A signal is a series of numbers or data that come from any measurement, typically obtained using some recording method as a function of time [15]. Many signals in nature exhibit random or nondeterministic characteristics which provide a challenge to analyse using signal processing techniques [16].

In actual applications, mechanical signals can be classified to have stationary or non-stationary behaviour. Stationary signal have the behaviour that the statistical property values remained unchanged with the changes in time. For non-stationary, however, the statistical parameter values of a signal are dependent to the time of measurement. For both stationary and non-stationary signal, the engineering-based signal analysis is important to explore the characteristics and behaviour of the

signal, and the outcomes of these can also related to the fault detection and analysis [17].

The global signal statistics are frequently used to classify random signals and the most commonly used statistical parameters are the mean value, the standard deviation value, the root-mean-square (r.m.s.) value, the skewness and the kurtosis [18].

Statistic analysis had been performed in order to achieve the objective of this paper. Both strain and vibration signals were analysed using the Hybrid I-kaz method, a new statistical-based method. The Hybrid I-kaz method was developed based on the concept of magnitude distribution about its centroid. This method provides a two dimensional graphical representation of the magnitude distribution. The Hybrid I-kaz coefficient, Z_h^{∞} was given as in Eq. (6)

$$Z_h^{\infty} = \frac{1}{N}\left(\sqrt{K_{\varepsilon} S_{\varepsilon}^{\ 4} + K_v S_v^{\ 4}}\right) \tag{6}$$

Where N is the number of data, K_{ε} and K_V are the kurtosis of the strain and vibration signal, respectively and S_{ε} and S_V are the standard deviation of the strain and vibration signals, respectively. The standard deviation (S) for n data point is mathematically defined as

$$S = \left\{\frac{1}{n}\sum_{j=1}^{n}\left(x_j - \bar{x}\right)^2\right\}^{\frac{1}{2}} \tag{7}$$

Kurtosis value was mathematically defined as Eq. (8). Kurtosis, which is the signal 4th statistical moment, is a global signal statistic which is highly sensitive to the spikiness of the data. Higher kurtosis values indicate the presence of more extreme values than should be found in a Gaussian distribution. Kurtosis is used in engineering for detection of fault symptoms because of its sensitivity to high amplitude events [19].

$$K = \frac{1}{n\left(r.m.s\right)^4}\sum_{j=1}^{n}\left(x_j - \bar{x}\right)^4 \tag{8}$$

3 Methodology

The Finite element analysis (FEA) has been performed in this work in order to determine the highest static stress position. This analysis was implemented using MSC. Patran and MSC. Nastran. The aim of the FEA is to identify the highest stress position for the placement of the strain gauge and accelerometer on the coil spring during the automobile road test. Thus, this study focuses on the specific position that is critical zone since this zone contributes to the fatigue failure of this component.

The selected material for the simulation testing purpose was the chromium steel, SAE5160. This material was chosen because it was commonly used to fabricate a coil spring for the vehicle suspension system. The material properties and their definitions are given in Table 1 and Fig. 1 shows the strain-life curve of this material type.

Table1: Mechanical Properties of the Chromium Steel, SAE 5160

Properties	Chromium steel, SAE 5160
Ultimate tensile strength, S_u (MPa)	1584
Modulus of elasticity, E (GPa)	207
Fatigue strength coefficient, σ'_f(MPa)	2063
Fatigue strength exponent, b	-0.08
Fatigue ductility exponent, c	-1.05
Fatigue ductility coefficient, ε'_f	9.56

Fig. 2 illustrates the critical stress zone experiencing by the automobile under static loading. The different colour contours in this figure indicates the different stress values were observed on this component. The red colour contour indicates the maximum stress that is at 240 MPa was observed at the inner surface. From this FEA observation, it was found that the inner coil surface is the most damaging zone compared to other surfaces.

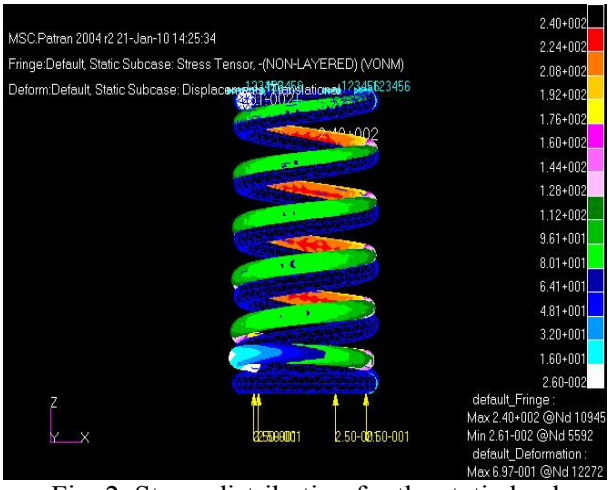

Fig. 2. Stress distribution for the static load

An actual road-load testing was conducted in order to validate the static FEA result. This is because this automobile was subjected to the cyclic loading under actual application. The measured strain loading was then used as the input information for the cyclic-based FEA calculation.

Because of the difficulty in sticking the strain gauge on an inner surface of the coil spring, the outer critical zone surface was chosen as the subject zone in this study as shown in Fig. 3. The car was then driven over the road for collecting the strain signal that will be used as the input for the cyclic FEA analysis. During the test, the car was constantly driven at 40 km/h on the damage-surface road surface.

The measured strain signal was shown in Fig. 4. On the other hand, Fig. 5 shows the obtained result for the FEA-based cyclic simulation, indicating the maximum critical stress for the inner and outer surfaces was in concordance to the result in Fig. 2. Therefore, the outer surface of the coil spring has been chosen for further analysis in this subject since it agreed with the static and cyclic simulation, in which it clearly contributed to the failure of an automobile component.

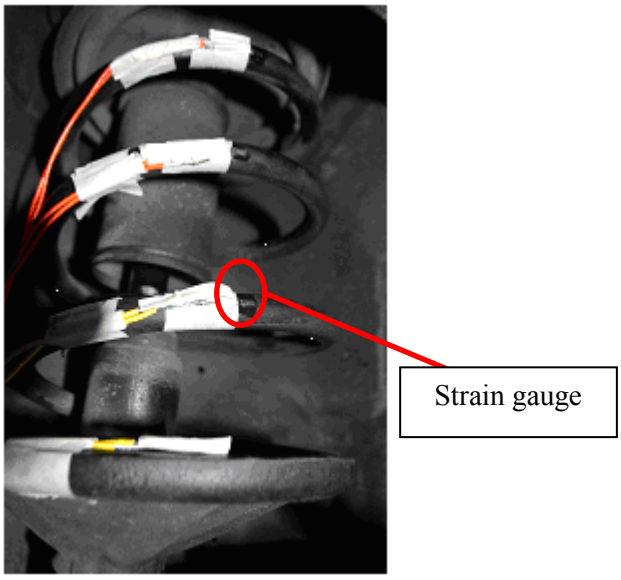

Fig. 3. Position of the strain gauge on the coil spring during the road test

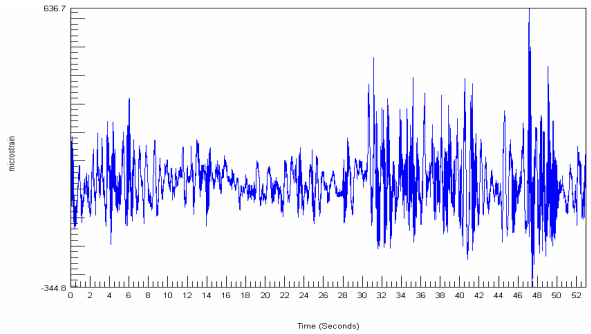

Fig. 4. The actual strain signal which is captured from the road test

The laboratory experiment was then carried out on the durability test rig, in which the rig was designed as a full scale of the automotive suspension system (see Fig. 6). The 5 mm strain gauge and the Endevco® model 751 accelerometer were mounted on the outer surface of the coil spring for capturing the strain and vibration signals respectively.

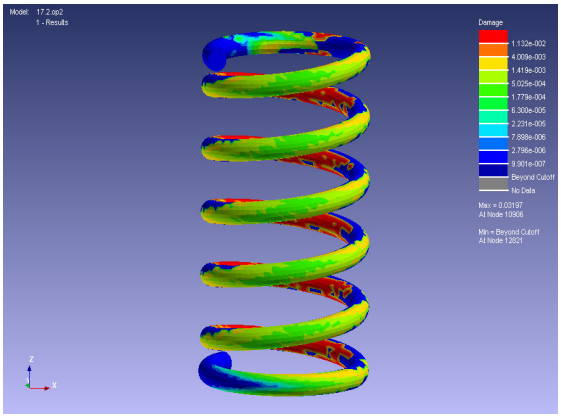

Fig. 5. FEA distribution of fatigue damage using the measured cyclic load

SoMat eDAQ Data Acquisition was used for the strain signal measurement and PXI System was used for the vibration response measurement. The main reason for capturing the strain and vibration signals was to determine the correlation between these two parameters that is the main objective of this paper.

Fig. 6. Durability test rig for laboratory data measurement.

During the laboratory test, 10 different frequencies were used as the excitations to the coil spring. The selected frequency values were varied from 1 Hz to 10 Hz. Frequency differences are important in this study since the recorded strain and vibration signals are needed for their correlation purposes. In the signal analyses, the fatigue damage assessment and the Hybrid I-kaz method were applied for each collected signal. Finally, the correlation analysis was then performed in term of

the total fatigue damage and Hybrid I-kaz coefficient and also the observation of the two dimensional graphical representation. All the previously discussed methodology can be seen in Fig. 7.

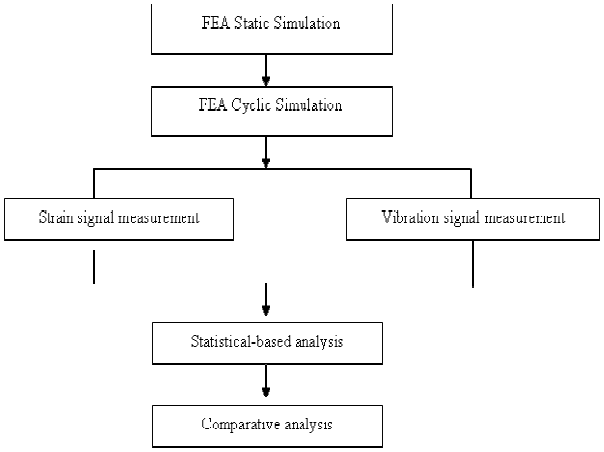

Fig. 6. The block diagram of the experimental process.

4 Results and Discussion

4.1 Time domain signal

The captured strain and vibration signals vary from 1 Hz to 10 Hz were then analysed in the time domain signals. The original time domain signal for strain and vibration signals were presented in Fig. 8 and Fig. 9, respectively. All the signals were sampled at 500 Hz for 60 seconds record length. Thus, the time series of 30,000 data points was then produced.

From Fig. 8 it shows clearly the highest frequency, 10 Hz, contributes the highest displacement to the coil spring, i.e. 205 με and then followed by 9 Hz, 8 Hz, 7 Hz, 6 Hz and 5 Hz. which were found at 184 με, 150 με, 132 με, 107 με 88.2 με, respectively. The lowest frequency that is 1 Hz gives the lowest displacement, which is at 6.6 με. The total strain ranges of the other frequencies were tabulated in Table 1. From the table, it shows the strain range of the strain signals were increased as the frequencies increase. Increments of the frequencies illustrate the increment of the total strain range. This situation was similar with the vehicle that was driven at the different velocity on the same road surface or condition. This indicates the automobile experiences higher shock at higher velocities compared to low velocities. This is because of a higher amount of load being transmitted to this component. The significant amount of this load will therefore, give the significant displacement to the coil spring.

The same case goes for the vibration signals. The highest total vibration amplitude was given by 10 Hz that is at 0.01 ms^{-2}. It was then followed by 9 Hz and 8 Hz which were found at 0.088 ms^{-2} and 0.08 ms^{-2}, respectively. The lowest frequency, 1 Hz was gave the lowest total vibration amplitude, i.e. 0.005 ms^{-2}. For the rest of the frequencies see Table 2. From these values, it show that the total vibrations amplitude were going higher with higher frequencies.

Thus, it clearly shows that the increments of the frequencies illustrate the increment of the vibration responses and the strain range.

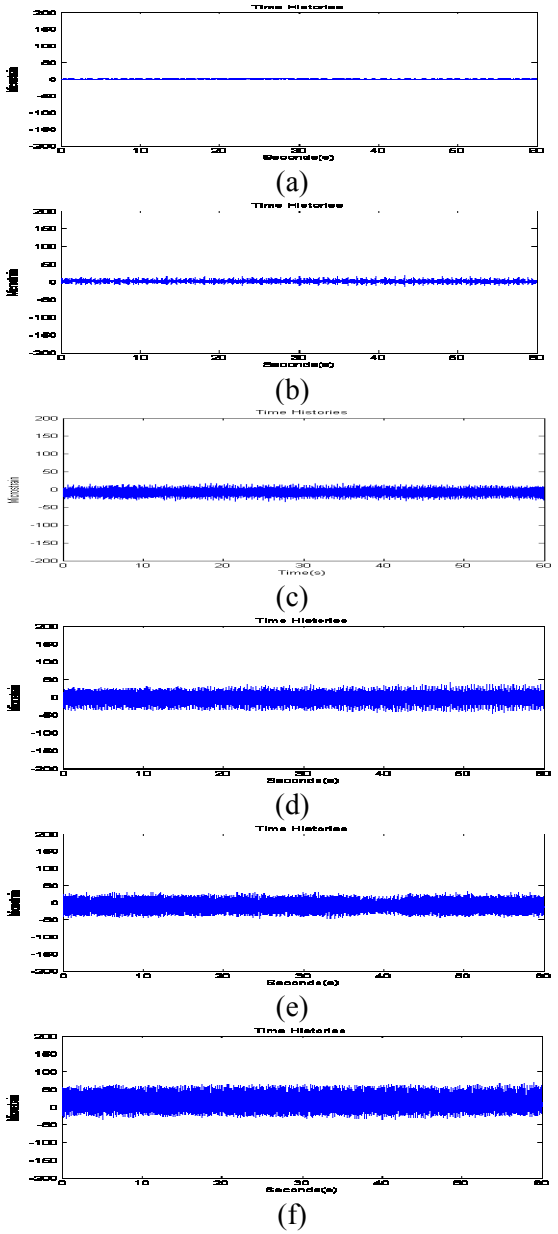

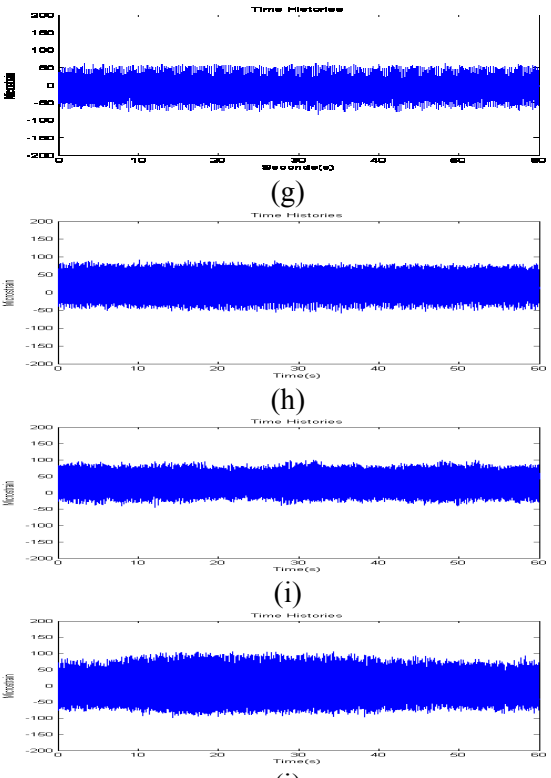

Fig. 8 The time series plots of the measured strain signal at different frequencies (a) 1 Hz, (b) 2 Hz, (c) 3 Hz, (d) 4 Hz, (e) 5 Hz, (f) 6 Hz, (g) 7 Hz, (h) 8 Hz, (i) 9 Hz and (j) 10 Hz

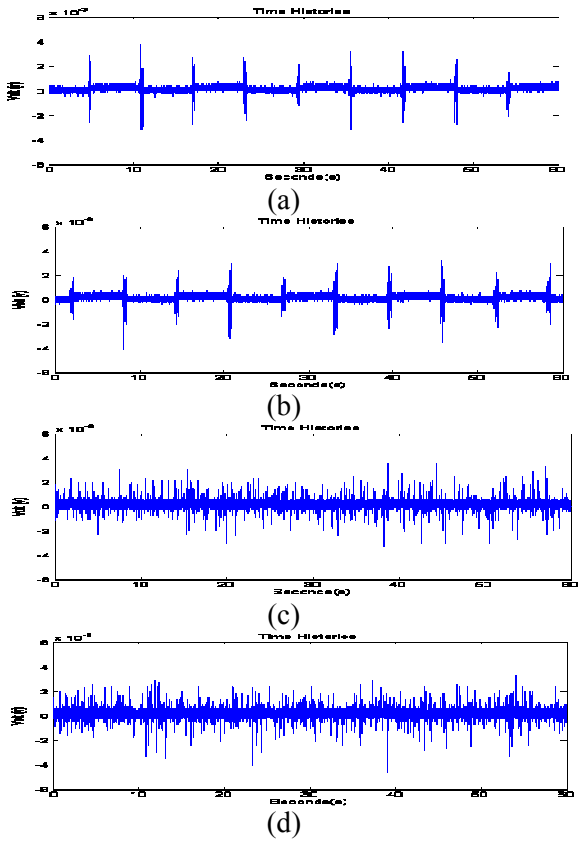

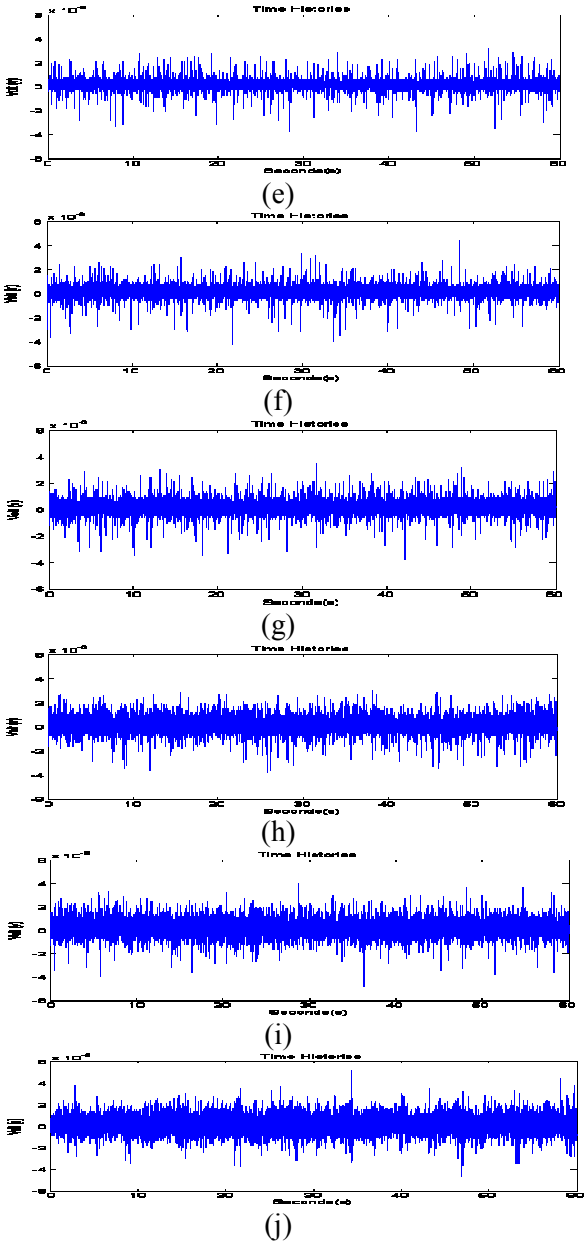

Fig. 9 The time series plots of the measured vibration signal at different frequencies (a) 1 Hz, (b) 2 Hz, (c) 3 Hz, (d) 4 Hz, (e) 5 Hz, (f) 6 Hz, (g) 7 Hz, (h) 8 Hz, (i) 9 Hz and (j) 10 Hz

4.2 Total Fatigue Damage Assessment, D

The first analysis that will be performed in this paper is the total fatigue damage assessment. Table 2 shows the results for the *D* after analysing using GlyphWorks® software and the strain signals as the input. This analysis was based on Coffin-Manson approach. Referring to Table 2, strain signal at 10 Hz produced the highest *D* which was found to be 4.6×10^{-1}. It was followed by 9Hz, 8 Hz and 7 Hz that is 5.5×10^{-2}, 3×10^{-2} and 2.8×10^{-2}, respectively.

According to the *D* value as tabulated in Table 3, the lower frequency illustrates the lower *D* value. It

Table 1: Total Strain Range and Total Vibration Amplitude of Each Frequency

Frequency (Hz)	Total Strain Range ($\mu\varepsilon$)	Total Vibration Amplitude (ms^{-2})
1	6.6	0.005
2	30.8	0.0053
3	48.8	0.0058
4	74.0	0.0063
5	88.2	0.0067
6	107.0	0.0070
7	132.0	0.0077
8	150.0	0.0082
9	184.0	0.0088
10	205.0	0.01

can be seen clearly at the lowest frequency that is 1 Hz does not contribute any damage to the coil spring. Automobile displacement at 1 Hz was too low compared to the other frequency. This is because the lower frequency gives smaller loading amplitude to this component and does not physically effect the coil spring. The *D* values for the rest of the frequencies can be seen in Table 2. All these values were agreed with the time domain signals in Fig. 8 and also with the total strain range values as shown in Table 2.

Table 2: Total Fatigue Damage of Each Frequency

Frequency (Hz)	*Total Fatigue Damage, D*
1	0
2	$9x10^{-9}$
3	$1.2x10^{-8}$
4	$4.8x10^{-5}$
5	$1.2x10^{-5}$
6	$5.0x10^{-3}$
7	$6.6x10^{-2}$
8	$7.8x10^{-2}$
9	$1.2x10^{-1}$
10	$6.0x10^{-1}$

4.3 Hybrid I-kaz Coefficient, Z_h^{∞}

In order to correlate the relationship between the strain and the vibration signals, a statistical analysis was implemented using the Hybrid I-kaz method. This method was utilised the strain and vibration signals of the input signal. The results obtained from the Hybrid I-kaz analysis for all signals were presented in Fig. 10, which illustrates the Hybrid I-kaz coefficient and two dimensional graphical representations of the amplitude distribution for the strain and vibration response signal.

From Fig. 10, the Hybrid I-kaz coefficient, Z_h^{∞} for 10 Hz was found to be the highest Z_h^{∞} value which was 0.072. It was then followed by 9 Hz, 8 Hz and 7 Hz at 0.0400, 0.0367 and 0.0277, respectively. The lowest frequency that is 1 Hz gave the lowest Z_h^{∞} value that was at 0.00002. Higher Z_h^{∞} value illustrates higher frequency that was applied to the coil spring. The obtained results were agreed with the *D* value that was tabulated in Table 3. In addition, this value was strongly supported by the observation on the space of scattering of Hybrid I-kaz display. This graphical representation shows the bigger space of scattering illustrates the Z_h^{∞} value of the signal was comparatively getting larger. The rest of the values of the Z_h^{∞} are simplified in Table 3.

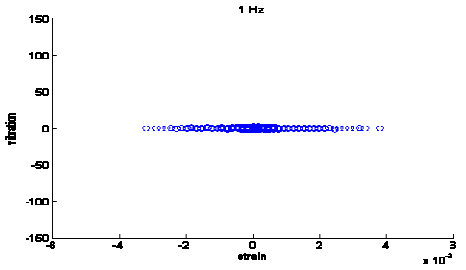

(a) Z_h^{∞}= 0.00002

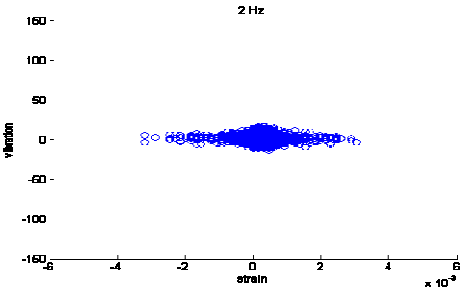

(b) Z_h^{∞}= 0.0006

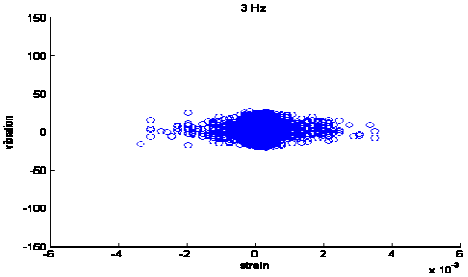

(c) Z_h^{∞}= 0.0029

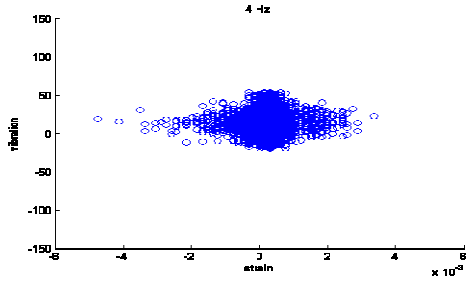

(d) Z_h^{∞}= 0.0061

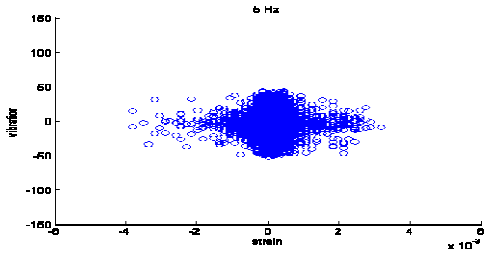

(e) Z_h^{∞}= 0.0108

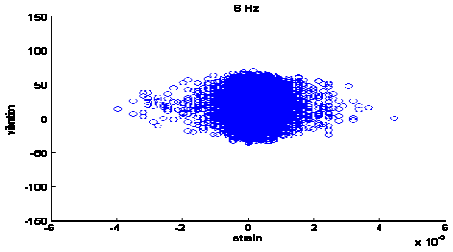

(f) Z_h^{∞} = 0.0174

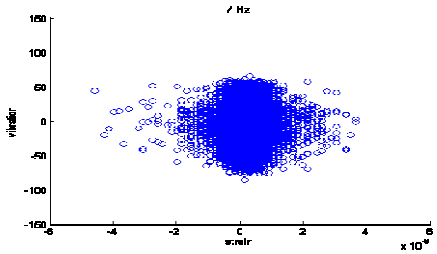

(g) Z_h^{∞}= 0.0277

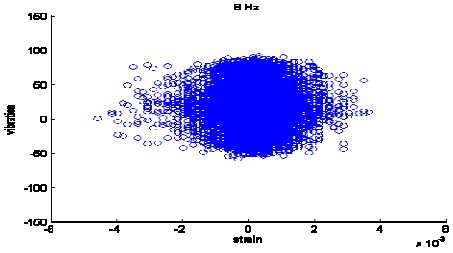

(h) Z_h^{∞}= 0.0367

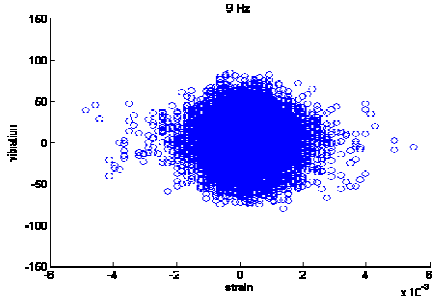

(i) Z_h^{∞}= 0.0400

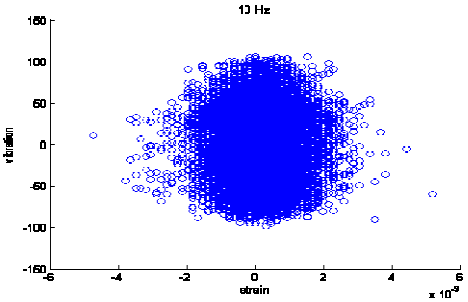

(j) Z_h^{∞}= 0.0720

Fig. 10 I-kaz Hybrid coefficient, Z_h^{∞} at the frequencies of (a) 1 Hz, (b) 2 Hz, (c) 3 Hz, (d) 4 Hz, (e) 5 Hz, (f) 6 Hz, (g) 7 Hz, (h) 8 Hz, (i) 9 Hz and (j) 10 Hz

From Table 3, it was obviously shown that the Z_h^{∞} value increased due to the increment of the frequency value. This relationship was supported by the statistical values as shown in Table 4 and Table 5. As mentioned before, the Hybrid I-kaz method was developed based on standard deviation and kurtosis which were mathematically defined as Eq. (6) and Eq. (7). As the frequency increased, the strain and vibration signal tend to have more spikiness rather than lower frequency. Higher kurtosis value indicates the presence of more extreme values.

Kurtosis of strain versus kurtosis of vibration was plotted in order to explain the reason to the increment of Z_h^{∞} as the frequency increased. Based on Fig. 11, it was clearly shown that kurtosis of the strain and vibration signal were linearly related to each other. In addition, similar results were obtained for the standard deviation of the strain signal when plotted against the standard deviation of the vibration signal, as shown in Fig. 12. It shows the standard deviation of the strain signal is also linear related to the standard deviation of the vibration signal. This absolutely proves why the Z_h^{∞} value increased as the frequency increased.

Table 3: Hybrid I-kaz coefficient, Z_h^{∞}

Frequency (Hz)	*I-kaz Hybrid Coefficient (Z_h^{∞})*
1	0.00002
2	0.0006
3	0.0029
4	0.0061
5	0.0108
6	0.0174
7	0.0277
8	0.0367
9	0.0400
10	0.0720

Table 4: Kurtosis values for the strain and vibration signal

Frequency (Hz)	*Kurtosis*	
	Strain signal	*Vibration signal*
1	1.0	1.8
2	1.5	2.1
3	1.7	2.5
4	2.5	2.7
5	3.2	3.3
6	3.7	4.1
7	4.1	4.9
8	4.6	6.0
9	5.9	6.8
10	6.1	7.3

Table 5: Kurtosis values for the strain and vibration signal

Frequency (Hz)	*Standard Deviation*	
	Strain signal	*Vibration signal($x10^{-4}$)*
1	8	1.5
2	10	2.1
3	14	2.8
4	16	3.0
5	17	3.4
6	19	3.6
7	22	4.4
8	25	4.7
9	28	5.6
10	30	6.6

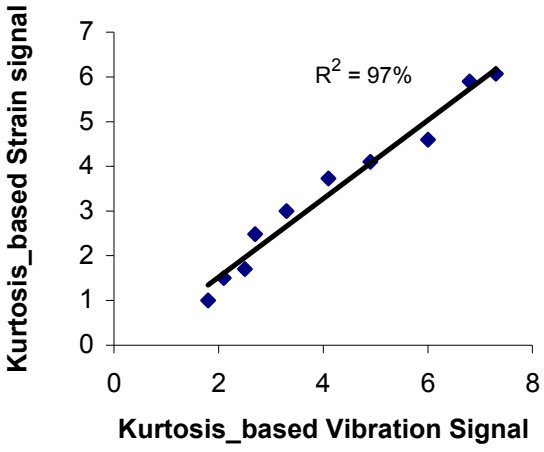

Fig. 11 Graph of Kurtosis of Strain Signal versus Kurtosis of Vibration Signal.

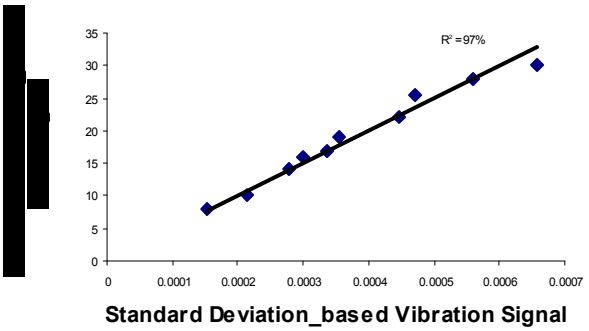

Fig. 12 Graph of Standard Deviation of Strain Signal versus Standard Deviation of Vibration Signal.

In order to achieve the objective of this paper, the total fatigue damage for each frequency was plotted versus the Hybrid I-kaz coefficient in logarithmic scale as shown in Fig. 13. Each data point represents the D and Z_h^{∞} value as tabulated in Table 2 and Table 3, respectively. The result shows the D value was linear proportionally related to the Z_h^{∞} value and mathematically derived as Eq. (9) and generally defined as Eq. (10). Constant α and β in Eq. (10) were varied based on the material and type of component used, respectively. Different material and type of component give the different value of constant α and β.

$$LogD = 1.6LogZ_h^{\infty} + 1.2 \quad (8)$$

$$D = 15.8\left(Z_h^{\infty}\right)^{1.6} \quad (9)$$

$$D = \alpha(Z_h^{\infty})^{\beta} \quad (10)$$

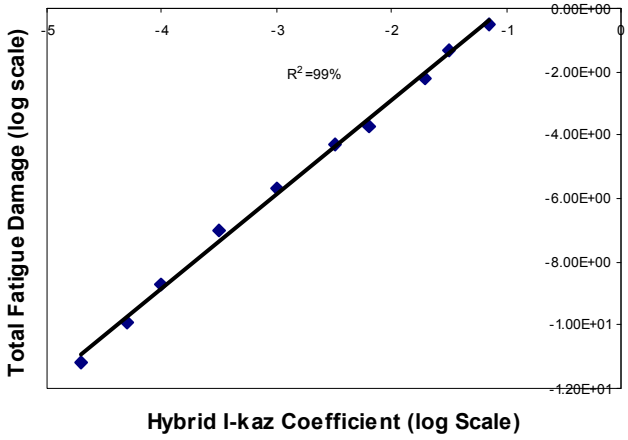

Fig. 13 Graph of Log Total Fatigue Damage Versus Log I-kaz Hybrid Coefficient

The mathematical equation in Eq. (10) was verified using the signals that were collected at the road test as shown in Fig. 14 and Fig. 15, indicating the strain signals and vibration signals, respectively. The actual road test used a coil spring that was made of similar material with the coil spring that was used for the laboratory testing.

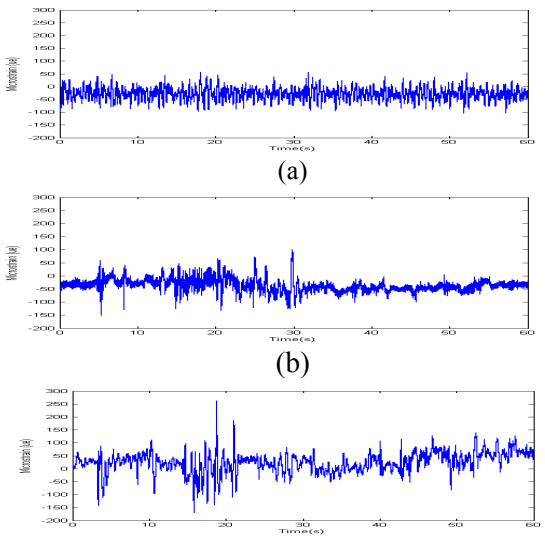

(a)

(b)

(c)

Fig. 14 The strain signal measured at (a) highway, (b) campus road (c) country road

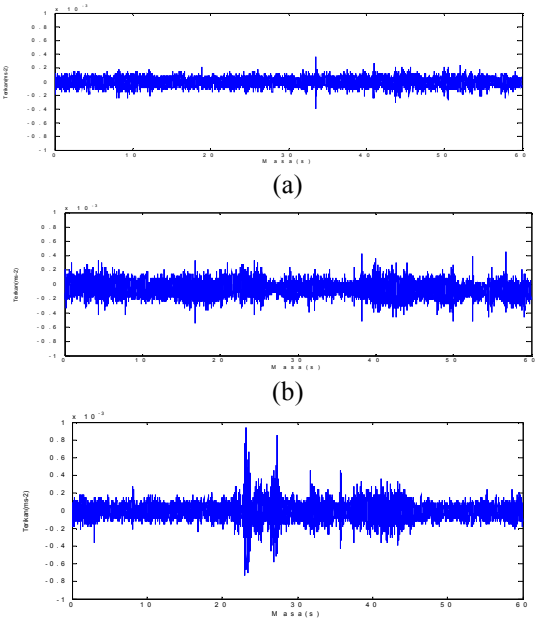

(a)

(b)

(c)

Fig. 15 The vibration signal measured at (a) highway, (b) campus road (c) country road

The same analyses has been implemented for these three signals that were the total fatigue damage assessment and the Hybrid I-kaz method. The reason for this statement is because the results obtained from these analyses were used to validate Eq. (9).

Table 6 shows the D values for highway, pave track and country road. From Table 6, the D value predicted using Glyphworks software of the country road, campus road and highway was found at 15.1 x 10^{-2}, 10 x 10^{-2} and 5.5 x 10^{-2}, respectively. While the D value calculated from the developed equation (Eq. 9) was given by 14.8 x 10^{-2}, 10.3 x 10^{-2} and 5.7 x 10^{-2} that refer to the country road, campus road and highway, respectively. The $\not{Z}_h^{\infty}$ values that were applied in the developed equation were shown in Fig. 16 together with the Hybrid I-kaz graphical representations.

Table 6: Total Fatigue Damage based on Glyphworks Software and Mathematical Equation

Type of Road	D (x10^{-2})		D Difference (%)
	Glyphworks	Equation	
Country road	15.1	14.8	2
campus road	10	10.3	3
Highway	5.5	5.7	3.6

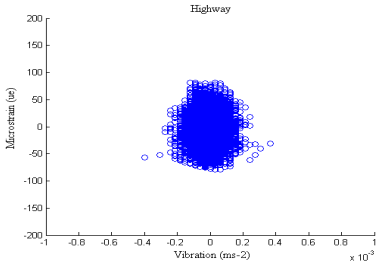

(a) $\not{Z}_h^{\infty}$= 0.03

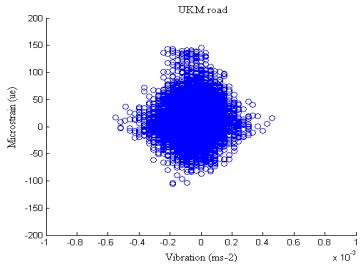

(b) $\not{Z}_h^{\infty}$= 0.044

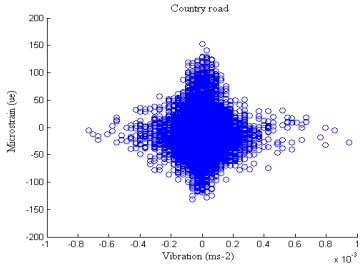

(c) $\not{Z}_h^{\infty}$= 0.054

Table 6 also shows the difference (in percent) between the predicted D using the developed equation and Glyphworks software. The difference was calculated as Eq. (11).

$$\frac{D_{equation} - D_{Glyphwork}}{D_{Glyphwork}} \text{X}100\% \qquad (11)$$

From Table 6, it can be seen that the fatigue damage difference for the country road, campus road and highway were found at 2 %, 3 % and 3.6 %, respectively. The small percentage for the total fatigue damage difference proved that the developed equation was valid for the same material and type of automobile that were used in the laboratory testing.

5 Conclusion

This paper discussed the comparative study of total fatigue damage and I-kaz Hybrid coefficient. The strain and vibration signals that were varied from 1 to 10 Hz were collected from the full scale automotive suspension system that was used as the subject of this study. A fatigue damage assessment of strain signal and I-kaz Hybrid method of strain and vibration signals was performed. From the analysis, the total fatigue damage was found to be linearly related to the I-kaz Hybrid coefficient as developed equation. The reason behind this statement is I-kaz Hybrid method in developed based on kurtosis and total fatigue damage has a relationship with kurtosis since kurtosis is used in engineering for detection of fault symptoms because of its sensitivity to high amplitude events. This result shows that, the developed equation can be used as the total fatigue damage prediction as an alternative method based on similar material and type of component.

References:

[1] S. Abdullah, M.Z. Nuawi, A. Zaharim, Application of a Computational Data Editing Algorithm to Summerise Fatigue Road loading, *WSEAS Transactions on Signal Processing, 2007,pp. 231-236.*

[2] X. B. Lin, & P. J. Heyes, Some Aspects of Automotive Durability Analysis, *Proceedings of the Seventh International Fatigue Congress*, edited by X. R. Wu, Z. G. Wang, Beijing, China. 1999.

[3] S. Abdullah, Wavelet Bump Extraction (WBE) for Editing Variable Amplitude Fatigue Loading. Thesis of Doctoral of Philosophy, University of Sheffield, United Kingdom. 2005

[4] R. I. Stephens, P. M. Dindinger & J.E. Gunger, Fatigue Damage Editing for Accelerated Durability Testing Using Strain Range and SWT Parameter Criteria, *Int. J. Fatigue*, Vol.19, 1997, pp. 599-606.

[5] L. Tucker & S. Bussa, The SAE cumulative fatigue damage test program, In Fatigue Under Complex Loading: Analysis and Experiments, edited by Wetzel, R. M., Warrendale, PA, Society of Automotive Engineers, 1977, pp. 3-14.

[6] S. D. Downing & D. F. Socie, Simple Rainflow Counting Algorithms, *Int. J. Fatigue*, Vol. 4, 1982, pp. 31-40.

[7] A. Conle & R. Landgraf, A Fatigue Analysis Program For Ground Vehicle Components, *Proceedings of International Conference on Digital Techniques in Fatigue*, London, 1983, pp 1-28.

[8] F. A. Conle & C. -C. Chu, Fatigue Analysis And The Local Stress-Strain Approach In Complex Vehicular Structures, *Int. J. Fatigue*, Vol. 19, Supp. No. 1, 1997, pp. S317-S323.

[9] C-C. Chu, Multiaxial Fatigue Life Prediction Method In The Ground Vehicle Industry, *Int. J. Fatigue*, Vol. 19, 1998, Supp. no.1, pp. S325-S330.

[10] N. E. Dowling, Mechanical Behaviour of Materials: Engineering Methods for Deformation, Fracture and Fatigue, Second Edition, Prentice Hall, New Jersey, 1999.

[11] L. F. Coffin, A Study of the Effect of Cyclic Thermal Stresses on a Ductile Metal, Transactions of ASME, Vol.79, 1954, pp. 931-950.

[12] S. S. Manson, Fatigue: A Complex Subject Some Simple Approximation. Experimental Mechanics, Vol. 5, 1965, pp.193-226.

13] J. D. Morrow, Fatigue Properties of Metal Fatigue Design Handbook, *Society of Automotive Engineers*, 1968.

[14] K. N. Smith, P. Watson & T. H. Topper, A Stress-Strain Function For The Fatigue of Metals, *Journal of Materials, JMLSA*, Vol. 5, 1970, pp. 767-778.

[15]Y. Meyer, Wavelets: Algorithm and Applications, *SIAM*, 1993, Philadelphia, USA.

[16] B. Tacer & P. J. Loughlin, Nonstationary Signal Classification Using the Joint Moments of Time-Frequency Distributions, *Pattern Recognition*, 31(1998), p. 1635-1641.

[17] J. Giacomin, A. Steinwolf and W. J. Staszewski in: A Vibration Mission Synthesis Algorithm for Mildly Nonstationary Road Data, *ATA 6th Int. Conf. on the New Role of Experimentation in the Modern Automotive Product Development Process*, Florence, Italy, 1999.

[18] P. R. Hinton, Statistics Explained: A Guide for Social Science Students, Routledge, London. 1995

[19] L. Qu, & Z. He, *Mechanical Diagnostics*, Shanghai Science and Technology Press, Shanghai, China. 1986.